Received: 3 February 2023 | Accepted: 2 May 2023

DOI: 10.1111/ene.15841

european journal of neurology
the official journal of the european academy of neurology

ORIGINAL ARTICLE

Peripheral nerve involvement in hereditary spastic paraplegia characterized by quantitative magnetic resonance neurography

Heike Jacobi[1] | Markus Weiler[1] | Georges Sam[1] | Sabine Heiland[2,3] | John M. Hayes[4] | Martin Bendszus[2] | Rebecca Schüle[1,5,6] | Jennifer C. Hayes[2]

[1]Department of Neurology, Heidelberg University Hospital, Heidelberg, Germany

[2]Department of Neuroradiology, Heidelberg University Hospital, Heidelberg, Germany

[3]Division of Experimental Radiology, Department of Neuroradiology, Heidelberg University Hospital, Heidelberg, Germany

[4]Department of Neurology, University of Michigan, Ann Arbor, Michigan, USA

[5]Center for Neurology and Hertie Institute for Clinical Brain Research, University Hospital, Tübingen, Germany

[6]German Center for Neurodegenerative Diseases (DZNE), Tübingen, Germany

Correspondence
Jennifer C. Hayes, Department of Neuroradiology, Heidelberg University Hospital, Im Neuenheimer Feld 400, Heidelberg D-69120, Germany.
Email: jennifer.hayes@med.uni-heidelberg.de

Heike Jacobi, Department of Neurology, Heidelberg University Hospital, Im Neuenheimer Feld 400, Heidelberg D-69120, Germany.
Email: heike.jacobi@med.uni-heidelberg.de

Funding information
Anylam Pharmaceuticals; Bundesministerium für Bildung und Forschung, Grant/Award Number: 01GM1905; Deutsche Forschungsgemeinschaft, Grant/Award Number: SFB 1118 and SFB 1158; Medizinischen Fakultät Heidelberg, Universität Heidelberg

Abstract

Background and objectives: Hereditary spastic paraplegias (HSPs) are heterogenous genetic disorders. While peripheral nerve involvement is frequent in spastic paraplegia 7 (SPG7), the evidence of peripheral nerve involvement in SPG4 is more controversial. We aimed to characterize lower extremity peripheral nerve involvement in SPG4 and SPG7 by quantitative magnetic resonance neurography (MRN).

Methods: Twenty-six HSP patients carrying either the SPG4 or SPG7 mutation and 26 age-/sex-matched healthy controls prospectively underwent high-resolution MRN with large coverage of the sciatic and tibial nerve. Dual-echo turbo-spin-echo sequences with spectral fat-saturation were utilized for T2-relaxometry and morphometric quantification, while two gradient-echo sequences with and without an off-resonance saturation rapid frequency pulse were applied for magnetization transfer contrast (MTC) imaging. HSP patients additionally underwent detailed neurologic and electroneurographic assessments.

Results: All microstructural (proton spin density [ρ], T2-relaxation time, magnetization transfer ratio) and morphometric (cross-sectional area) quantitative MRN markers were decreased in SPG4 and SPG7 indicating chronic axonopathy. ρ was superior in differentiating subgroups and identifying subclinical nerve damage in SPG4 and SPG7 without neurophysiologic signs of polyneuropathy. MRN markers correlated well with clinical scores and electroneurographic results.

Conclusions: MRN characterizes peripheral nerve involvement in SPG4 and SPG7 as a neuropathy with predominant axonal loss. Evidence of peripheral nerve involvement in SPG4 and SPG7, even without electroneurographically manifest polyneuropathy, and the good correlation of MRN markers with clinical measures of disease progression, challenge the traditional view of the existence of HSPs with isolated pyramidal signs and suggest MRN markers as potential progression biomarkers in HSP.

KEYWORDS
electrophysiology, hereditary spastic paraplegia, magnetic resonance neurography (MRN), magnetization transfer contrast imaging, T2-relaxometry

INTRODUCTION

Hereditary spastic paraplegias (HSPs) are a heterogeneous group of rare genetic disorders characterized by length-dependent axonal degeneration of the corticospinal tract and posterior columns leading to progressive weakness and spasticity of the lower limbs. All modes of inheritance and more than 80 different genes have been described [1]. Clinically, HSPs are classified as either pure or complex phenotypes [2–4]. Pure HSPs show nearly isolated pyramidal signs that may be accompanied by mild sensory abnormalities of the lower limbs, sphincter disturbances, pes cavus, and mild cognitive decline [2, 5]. Spastic paraplegia 4 (SPG4) is the most common form of autosomal-dominant inherited pure HSP, comprising up to 45% of all HSP cases [6].

In complex phenotypes, HSP may be associated with a large variability of neurologic and non-neurologic symptoms including cerebellar signs, peripheral neuropathy, pale optic discs, amyotrophy, movement disorders, or mental retardation [5]. SPG7 is typically inherited in an autosomal-recessive mode, and can manifest with pure or complicated HSP phenotypes [5]. While peripheral nerve involvement is frequent in SPG7, it is more controversially discussed in SPG4 [7–9].

In recent years, quantitative magnetic resonance neurography (MRN) has been used to detect and localize peripheral nerve lesions in vivo in different diffuse neuropathies and motor neuron diseases [10–14]. With this study, we aimed to characterize lower extremity peripheral nerve lesions by applying MRN in genetically, clinically, and electrophysiologically classified HSP patients carrying either the SPG4 or SPG7 mutation. Nerve lesion quantification was performed by T2-relaxometry, magnetization transfer contrast (MTC) imaging, and morphometric quantification.

METHODS

Study design, neurologic, and electrophysiologic assessments

Approval from the institutional ethics board (University of Heidelberg; S-398/2012) was received for this prospective case–control study, and written informed consent was obtained from all participants.

A total of 26 HSP patients were enrolled from July 2019 to September 2021. Among them, 16 patients carried mutations in the SPG4-gene (SPAST) (seven males, nine females, mean age 53.3 ± 3.3 years), while 10 patients carried biallelic SPG7 mutations (eight males, two females, mean age 53.2 ± 3.3 years). We also recruited 26 age- and sex-matched healthy volunteers (15 males, 11 females, mean age 52.8 ± 2.1 years). Exclusion criteria were age < 18 years, pregnancy, any contraindications for magnetic resonance imaging (MRI), prior treatments with potentially neurotoxic agents, concomitant causes for polyneuropathy (PNP) development such as diabetes mellitus, severe hypothyroidism, or Vitamin B12 deficiency, as well as any malignant or infectious diseases or neurologic disorders other than HSP.

A detailed neurologic examination was performed in each patient including assessment of the severity of spastic paraplegia by using the Spastic Paraplegia Rating Scale (SPRS) [15], and testing for pallhypesthesia. Nerve conduction studies assessed distal motor latencies (DML), compound muscle action potentials (CMAPs), and nerve conduction velocities (NCVs) of the right peroneal and left tibial nerves. Sensory nerve action potentials (SNAPs) and NCVs were measured for the right and left sural nerves.

A diagnosis of PNP in our HSP patients was solely defined based on electroneurographic results without accounting for clinical presentations, requiring either pathologic CMAP or SNAP amplitudes in at least two different leg nerves. This procedure was favored to reduce the risk that potentially overlapping clinical symptoms caused by the degeneration of the corticospinal tract and posterior column might be viewed as signs of PNP.

Magnetic resonance neurography (MRN)

All participants were examined supine and feet first with a 15-channel transmit-receive extremity-coil (INVIVO) in a 3.0 Tesla MR-scanner (Magnetom PRISMA, Siemens-Healthineers) by applying a high-resolution MRN protocol for T2-relaxometry and MTC imaging as described elsewhere (for full MRN protocol see Data S1) [14]. The approximate total imaging time for this protocol including survey scans as well as patient and coil repositioning was 75 min.

Image analysis

After pseudonymization, all images were analyzed in ImageJ (version 1.52v; National Institutes of Health) by one neuroradiologist blinded to clinical data. For T2-relaxometry, the tibial nerve and respective tibial fascicles within the sciatic nerve were manually segmented on 20 central slices of each of the four imaging slabs generated by a T2-relaxometry sequence from the left proximal thigh down to the left tibiotalar joint (totaling 80 segmented slices per participant). Additional 20 central slices were segmented from one imaging slab acquired at the right mid- to distal thigh to account for potential side differences. Subsequently, the apparent T2-relaxation time ($T2_{app}$, Equation 1) and proton spin density (ρ, Equation 2) were calculated by using data from the T2-relaxometry sequence with SI = signal, $TE_1 = 14$ ms, and $TE_2 = 86$ ms [16, 17].

$$T2app = \frac{TE_2 - TE_1}{\ln\left(\frac{SI(TE1)}{SI(TE2)}\right)} \quad (1)$$

$$\rho = \frac{SI(TE_1)}{\exp\left(\frac{TE_1}{T2_{app}}\right)} \quad (2)$$

After calculating mean values of tibial nerve ρ and $T2_{app}$ per slice position for each participant, mean ρ, and $T2_{app}$ values were averaged for the thigh and the lower leg.

Tibial nerve cross-sectional area (CSA) was evaluated by using the exact same regions of interest on the same 20 central slices that were segmented for T2-relaxometry.

For MTC imaging, the sciatic nerve was manually delineated on 10 central slices generated by a gradient echo sequence without an off-resonance saturation pulse at the right mid- to distal thigh, with subsequent transfer of each respective region of interest to the exact same position on the corresponding slices generated by the sequence with an off-resonance saturation pulse. The magnetization transfer ratio (MTR) was first calculated separately for each evaluated imaging slice according to the following equation (S_0 = signal without, S_1 = signal with the off-resonance saturation pulse), and was subsequently averaged over the 10 slice positions analyzed in each participant.

$$MTR = 100 \times \frac{(S_0 - S_1)}{S_0} \quad (3)$$

Image postprocessing, nerve segmentation, and calculation of respective quantitative MRN markers required approximately 45 min per participant.

Statistical analyses

Statistical analyses were performed in GraphPad Prism (Version 9.3.1; GraphPad Software). Normal distribution of each quantitative dataset was confirmed by using the Kolmogorov–Smirnov test. Differences between SPG4, SPG7, and controls as well as between SPG4 PNP+, SPG4 PNP−, and controls were analyzed by using a one-way ANOVA for a priori assumptions, followed by post hoc analyses using the Tukey–Kramer test to correct for multiple comparisons and unequal sample sizes. Differences between the left and right distal thigh, as well as between the thigh and the lower leg, were evaluated by an unpaired *t*-test with Welch's correction. Correlation analyses between MRN parameters and demographic (age, sex, height, weight, body mass index), clinical (duration of symptoms, SPRS, pallhypesthesia), and electroneurographic (tibial and peroneal NCV, DML, and CMAP, sural nerve NCV, and SNAP) results were performed by calculating Pearson's correlation coefficients. Values of $p \leq 0.05$ were regarded as statistically significant. Results are documented as mean values ± standard error of the mean.

The data that support the findings of this study are available from the corresponding author upon reasonable request.

RESULTS

Clinical and electrophysiologic data

Seven of the 16 SPG4 patients and none of the SPG7 patients fulfilled the electroneurographic criteria for PNP. There were no differences in age or the SPRS score between SPG4 patients with and without PNP. Detailed demographic, clinical, and electrophysiologic characteristics of all participants are given in Table 1.

Magnetic resonance neurography (MRN) data

Proton spin density (ρ)

One-way ANOVA identified marked differences in tibial nerve ρ between SPG4, SPG7, and controls at the thigh ($p < 0.0001$, $F = 13.85$) and lower leg ($p < 0.0001$, $F = 20.96$). At both anatomic locations, subsequent post hoc analyses revealed a marked decrease of ρ in SPG4 and SPG7 versus controls (Table 2 and Figures 1a,b, and 2). When subdividing the SPG4 group into SPG4 PNP+ and SPG4 PNP−, ANOVA revealed group differences in tibial nerve ρ at the thigh ($p < 0.0001$, $F = 15.43$; Figure 1a) and lower leg ($p < 0.0001$, $F = 15.62$; Figure 1b). In detail, ρ was lower in SPG4 PNP+ and SPG4 PNP− versus controls, while differences between SPG4 PNP+ and SPG4 PNP− were not detected (Table 2).

A proximal-to-distal gradient with higher tibial nerve ρ at the thigh versus the lower leg was found in SPG4 ($p = 0.0223$) and SPG7 ($p = 0.0168$), but not in controls ($p = 0.14$). Differences between left and right mid- to distal thigh were absent in SPG4 ($p = 0.54$), SPG7 ($p = 0.72$), and controls ($p = 0.84$).

An inverse correlation was detected between tibial nerve ρ and the SPRS in SPG4 (thigh: $r = -0.4411$, $p = 0.0188$; lower leg: $r = -0.4397$, $p = 0.0133$). No further correlations were found.

Apparent T_2-relaxation time ($T2_{app}$)

Tibial nerve $T2_{app}$ at thigh level did not differ between SPG4, SPG7, and controls ($p = 0.12$, $F = 2.21$; Figure 1c), while ANOVA detected group differences at the lower leg ($p = 0.0385$, $F = 3.369$; Figure 1d). Here, $T2_{app}$ was lower in SPG7 versus controls, while differences between SPG4 and controls as well as between SPG4 and SPG7 were not observed (Table 2). Differences between SPG4 PNP+, SPG4 PNP−, and controls were absent for tibial nerve $T2_{app}$ at the lower leg ($p = 0.32$; $F = 1.156$; Figure 1d). A proximal-to-distal gradient in tibial nerve $T2_{app}$ did not exist in either group (SPG4: $p = 0.17$; SPG7: $p = 0.11$; controls: $p = 0.05$). Side differences in $T2_{app}$ did not exist in SPG4 ($p = 0.83$), SPG7 ($p = 0.96$), and controls ($p = 0.59$).

In SPG4, tibial nerve $T2_{app}$ at the thigh inversely correlated with the SPRS ($r = -0.4096$, $p = 0.0304$), disease duration ($r = -0.6948$, $p < 0.0001$), presence of PNP ($r = -0.3995$, $p = 0.0352$), and severity of pallaesthesia ($r = -0.5478$, $p = 0.0025$), while it positively correlated with NCVs of the peroneal (right: $r = 0.4067$, $p = 0.0317$; left: $r = 0.3998$, $p = 0.0351$), tibial (right: $r = 0.4709$, $p = 0.0114$; left: 0.4289, $p = 0.0228$), and sural nerve (right: $r = 0.4236$, $p = 0.0277$; left: $r = 0.4920$, $p = 0.0091$). At the lower leg, $T2_{app}$ inversely correlated with the SPRS ($r = -0.5424$, $p = 0.0016$) and disease duration ($r = -0.4483$, $p = 0.0114$) in SPG4; positive correlations were found for sural NCVs (right: $r = 0.4809$, $p = 0.0083$; left: $r = 0.4559$,

TABLE 1 Demographic, clinical, and electroneurographic data.

Parameter	SPG4 ($n=16$)	SPG7 ($n=10$)	SPG4 PNP+ ($n=7$)	SPG4 PNP− ($n=9$)	*P* value SPG4 PNP+ vs. SPG4 PNP−
Age (years)	53.3 ± 3.3	53.2 ± 3.3	52.9 ± 7.0	53.7 ± 2.7	0.92 (NS)
Sex (M/F)	7/9	8/2	5/2	2/7	NA
Body weight (kg)	76.2 ± 3.8	75.4 ± 4.1	84.6 ± 6.1	70.0 ± 3.9	0.06 (NS)
Height (cm)	171.7 ± 2.0	177.1 ± 2.5	175.1 ± 1.9	169.0 ± 3.1	0.12 (NS)
Body mass index (kg/m^2)	25.7 ± 0.9	23.9 ± 1.0	27.5 ± 1.8	24.2 ± 0.6	0.12 (NS)
SPRS (0–52 points)	18.5 ± 2.9	13.6 ± 1.2	14.9 ± 4.3	21.3 ± 3.9	0.28 (NS)
Weakness of hip abduction (none/mild/moderate/severe/plegia)	7/4/5/0/0	6/4/0/0/0	4/1/2/0/0	3/3/3/0/0	NA
Weakness of foot dorsiflexion (none/mild/moderate/severe/plegia)	8/7/0/0/1	8/2/0/0/0	5/2/0/0/0	3/5/0/0/1	NA
Ambulation (ambulant/walking aid/wheel chair)	9/4/3	8/2/0	4/2/1	5/2/2	NA
Disease duration	20.8 ± 3.4	15.3 ± 1.8	23.6 ± 6.2	18.7 ± 3.7	0.51 (NS)
Pallhypesthesia (none/mild/moderate/severe)	2/4/8/2	2/1/7/0	1/0/4/2	1/4/4/0	NA
PTR areflexia/normal/hyperreflexia	0/0/16	0/1/9	0/0/7	0/ 0/9	NA
ATR areflexia/normal/hyperreflexia	2/2/12	1/3/6	1/1/5	1/1/7	NA
SNAP (μV)					
RSN	10.4 ± 1.4	13.0 ± 2.4	5.3 ± 0.7	13.8 ± 1.3	0.0001[b]
LSN	9.2 ± 1.2	11.7 ± 1.6	5.4 ± 1.0	11.7 ± 1.3	0.0021[a]
CMAP (mV)					
RPN	6.3 ± 0.8	6.4 ± 0.7	6.7 ± 1.5	6.1 ± 0.9	0.75 (NS)
LPN	6.0 ± 0.7	6.9 ± 0.8	6.3 ± 1.3	5.8 ± 0.8	0.72 (NS)
RTN	13.4 ± 1.4	14.1 ± 1.8	10.7 ± 1.7	15.4 ± 1.9	0.09 (NS)
LTN	14.1 ± 1.6	15.9 ± 2.2	9.6 ± 1.2	17.6 ± 2.0	0.0050[a]
DML (ms)					
RPN	4.0 ± 0.1	4.0 ± 0.2	3.9 ± 0.2	4.0 ± 0.2	0.62 (NS)
LPN	3.9 ± 0.2	4.0 ± 0.1	4.0 ± 0.1	3.9 ± 0.3	0.60 (NS)
RTN	3.7 ± 0.2	3.4 ± 0.1	3.7 ± 0.2	3.7 ± 0.2	0.83 (NS)
LTN	3.6 ± 0.1	3.6 ± 0.1	3.5 ± 0.2	3.7 ± 0.1	0.55 (NS)
NCV (m/s)					
RPN	46.7 ± 1.2	47.2 ± 0.8	45.7 ± 2.0	47.4 ± 1.4	0.52 (NS)
LPN	47.4 ± 1.1	47.2 ± 1.3	47.2 ± 1.4	47.5 ± 1.6	0.91 (NS)
RTN	48.3 ± 1.0	48.2 ± 1.2	48.7 ± 1.4	48.0 ± 1.4	0.73 (NS)
LTN	49.1 ± 0.8	47.8 ± 0.9	48.7 ± 1.4	49.3 ± 1.0	0.75 (NS)
RSN	49.8 ± 1.0	51.4 ± 1.3	50.4 ± 1.4	49.5 ± 1.5	0.67 (NS)
LSN	50.6 ± 1.1	50.1 ± 1.6	50.6 ± 1.1	50.6 ± 1.7	0.98 (NS)

Note: All results are presented as mean values ± standard error of the mean.

Abbreviations: 0, no weakness (Medical Research Council [MRC] Scale 5/5); 1, mild weakness (MRC 4/5); 2, moderate weakness (MRC 3/5); 3, severe weakness (MRC 1–2/5); 4, plegia (MRC 0/5); ATR, Achilles tendon reflex; CMAP, compound muscle action potential; DML, distal motor latency; LPN, left peroneal nerve; LSN, left sural nerve; LTN, left tibial nerve; NA, not applicable; NCV, nerve conduction velocity; NS, not significant; pallhypesthesia tested at the external malleolus: none = 8/8, mild ≥ 5/8, moderate = 2–5/8, severe ≤ 2/8; PTR, patellar tendon reflex; RPN, right peroneal nerve; RSN, right sural nerve; RTN, right tibial nerve; SNAP, sensory nerve action potential; SPG4 PNP−, spastic paraplegia type 4 patients without polyneuropathy; SPG4 PNP+, spastic paraplegia type 4 patients with polyneuropathy; SPG4, spastic paraplegia type 4 patients; SPG7, spastic paraplegia type 7 patients; SPRS, spastic paraplegia rating scale; motor strength.

[a]Significant ($p \leq 0.05$).

[b]Highly significant ($p \leq 0.001$).

TABLE 2 Quantitative magnetic resonance neurography data.

Parameter	SPG4	SPG7	Controls	*P* value SPG4 vs. controls	*P* value SPG7 vs. controls	*P* value SPG4 vs. SPG7	SPG4 PNP+	SPG4 PNP−	*P* value SPG4 PNP+ vs. controls	*P* value SPG4 PNP− vs. controls	*P* value SPG4 PNP− vs. SPG4 PNP−
ρ (AU)											
Thigh	383.2 ± 11.7	407.0 ± 18.5	465.7 ± 10.0	<0.0001[b]	0.0071[a]	0.84 (NS)	362.3 ± 16.3	398.8 ± 15.7	<0.0001[b]	0.0018[a]	0.30 (NS)
Lower leg	343.6 ± 12.1	348.9 ± 13.6	442.7 ± 11.8	<0.0001[b]	<0.0001[b]	0.99 (NS)	333.2 ± 15.8	352.2 ± 18.0	<0.0001[b]	0.0003[b]	0.78 (NS)
$T2_{app}$ (ms)											
Thigh	NA	NA	NA	NA	NA	NA	NA	NA	NA	NA	NA
Lower leg	62.4 ± 1.4	59.1 ± 1.7	64.2 ± 1.0	0.51 (NS)	0.0306[a]	0.28 (NS)	NA	NA	NA	NA	NA
MTR (%)											
Thigh	29.9 ± 0.8	29.1 ± 1.1	32.4 ± 0.5	0.0406[a]	0.0101[a]	0.77 (NS)	28.2 ± 0.8	31.3 ± 1.0	0.0022[a]	0.59 (NS)	0.07 (NS)
CSA (mm^2)											
Thigh	12.1 ± 0.4	12.9 ± 0.6	13.6 ± 0.3	0.0184[a]	0.52 (NS)	0.45 (NS)	11.7 ± 0.6	12.4 ± 0.6	0.0192[a]	0.15 (NS)	0.63 (NS)
Lower leg	5.6 ± 0.3	6.0 ± 0.3	7.4 ± 0.2	<0.0001[b]	0.0016[a]	0.67 (NS)	5.5 ± 0.5	5.8 ± 0.3	0.0002[b]	0.0005[b]	0.89 (NS)

Note: All results are presented as mean values ± standard error of the mean.

Abbreviations: AU, arbitrary unit; CSA, cross-sectional area; MTR, magnetization transfer ratio; NA, not applicable; NS, not significant; SPG4 PNP−, spastic paraplegia type 4 patients without polyneuropathy; SPG4 PNP+, spastic paraplegia type 4 patients with polyneuropathy; SPG4, spastic paraplegia type 4 patients; SPG7, spastic paraplegia type 7 patients; T2app, apparent T2-relaxation time; ρ, proton spin density.

[a]Significant ($p \leq 0.05$).

[b]Highly significant ($p \leq 0.001$).

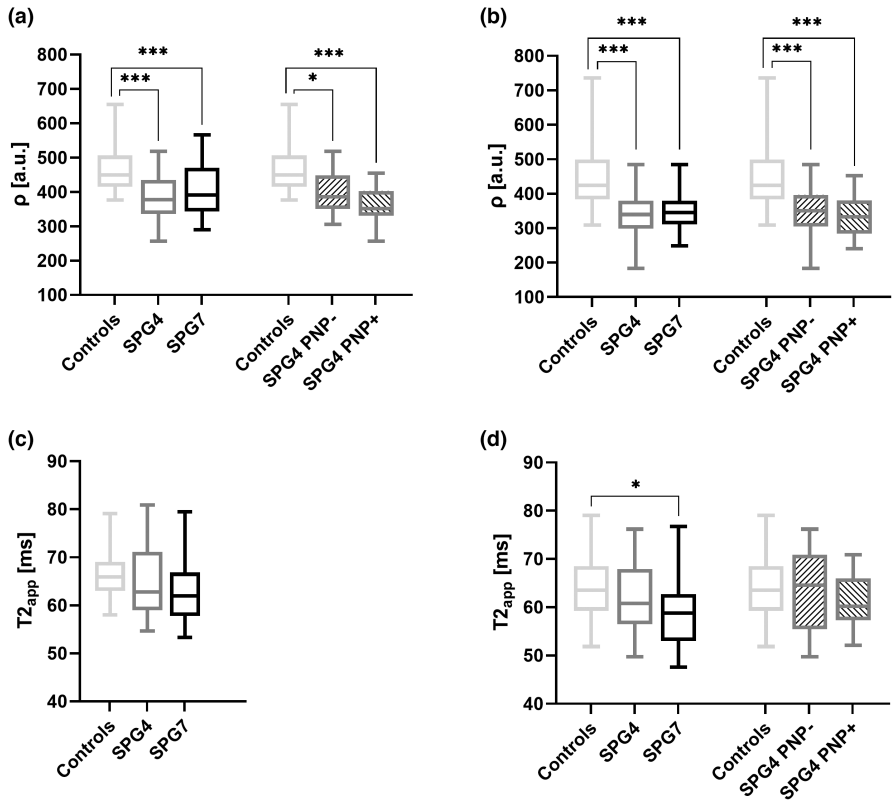

FIGURE 1 Proton spin density (ρ) and T2-relaxation time. Mean values of tibial nerve ρ (a, b), and $T2_{app}$ (c, d) were plotted separately for each group at the thigh (a, c) and at the lower leg (b, d) in a box and whisker plot. ρ differentiated well between healthy controls and SPG4 as well as between controls and SPG7 patients at the thigh (a) and at the lower leg (b). After subdividing the SPG4 group into patients with and without PNP, ρ was higher in SPG4 with PNP but also in SPG4 without PNP compared to healthy controls at both anatomic locations (a, b). As no differences in $T2_{app}$ between controls, SPG4, and SPG7 were found at the thigh (c), we did not further subdivide the group of SPG4 patients into patients with and without PNP. At the lower leg, $T2_{app}$ distinguished SPG7 patients from healthy controls, while all other group differences were insignificant (d). SPG4, spastic paraplegia 4 patients; SPG4 PNP−, spastic paraplegia type 4 patients without polyneuropathy; SPG4 PNP+, spastic paraplegia type 4 patients with polyneuropathy; SPG7, spastic paraplegia type 7 patients; $T2_{app}$, apparent T2-relaxation time; ρ, proton spin density. Significant differences are indicated by either * = significant ($p \leq 0.05$) or *** = highly significant ($p \leq 0.001$).

$p = 0.0129$). In SPG7, tibial nerve $T2_{app}$ at thigh level correlated positively with tibial nerve CMAPs (right: $r = 0.5409$, $p = 0.0205$; left: $r = 0.5986$, $p = 0.0087$), and sural nerve SNAPs (right: $r = 0.7370$, $p = 0.0005$; left: $r = 0.6496$, $p = 0.0035$), while at the lower leg, positive correlations were only found for sural nerve SNAPs (right: $r = 0.6018$, $p = 0.0082$, left: $r = 0.6774$, $p = 0.0020$).

Magnetization transfer ratio (MTR)

Sciatic nerve MTR at the right thigh was markedly different between SPG4, SPG7, and controls ($p = 0.0055$, $F = 5.929$). In detail, MTR was reduced in SPG4 and SPG7 versus controls (Table 2 and Figures 3 and 4), while differences between SPG4 and SPG7 were not detected. One-way ANOVA revealed marked differences between SPG4 PNP+, SPG4 PNP−, and controls ($p = 0.0033$; $F = 6.926$). In detail, MTR values were lower in SPG4 PNP+ than in controls ($p = 0.0022$), but did not differ between SPG4 PNP− and controls or between SPG4 PNP+ and SPG4 PNP− (Table 2 and Figure 3).

In healthy controls, sciatic nerve MTR showed an inverse correlation with age ($r = -0.5036$; $p = 0.0143$). In SPG4, MTR correlated inversely with age ($r = -0.7214$, $p = 0.0054$) and positively with sural nerve NCVs (right: $r = 0.7403$, $p = 0.0059$; left: $r = 0.8252$, $p = 0.0010$). In SPG7, inverse correlations were found between MTR and age ($r = -0.7678$, $p = 0.0095$), while positive correlations were identified with sural nerve SNAPs ($r = 0.7836$, $p = 0.0073$).

Cross-sectional area (CSA)

One-way ANOVA detected clear differences of tibial nerve CSA between SPG4, SPG7, and controls at thigh ($p = 0.0247$, $F = 3.863$) and lower leg level ($p < 0.0001$, $F = 16.61$; Figure 2). At thigh level, tibial nerve CSA was lower in SPG4 versus controls, but did not differ between SPG7 and controls or between SPG4 and SPG7 (Table 2 and Figure 5a). Tibial nerve CSA at the lower leg was reduced in both SPG4 and SPG7 versus controls, while differences between SPG4 and SPG7 were absent (Table 2 and Figure 5b). After subdividing

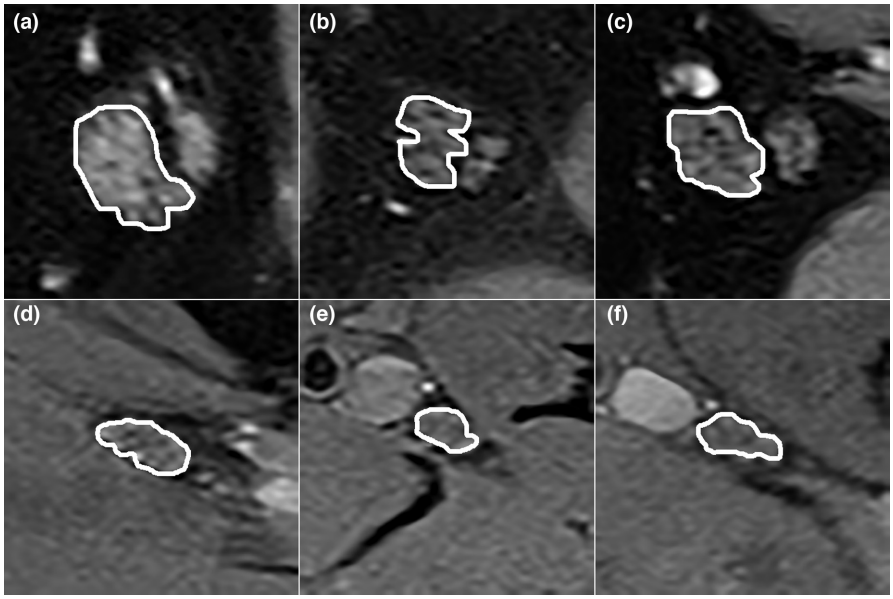

FIGURE 2 Magnetic resonance neurography (MRN) source images. Representative MRN images (axial dual-echo turbo spin echo relaxometry sequences with spectral fat saturation) at the left midthigh (a–c) and at the lower leg (d–f) are shown at equal slice positions in a healthy control (a, d), a SPG4 patient (b, e), and a SPG7 patient (c). The tibial fascicles within the sciatic nerve (a–c) as well as the respective tibial nerve (d–f) are encircled in white. Note the slight decrease in tibial fascicle and tibial nerve T2w signal, a consequence of the decrease in both ρ and $T2_{app}$, in SPG4 (b, e) and SPG7 (c, f) compared to the healthy control (a, d). Tibial fascicle CSA in SPG4 (b) as well as tibial nerve CSA in SPG 4 (e) and SPG7 (f) was also decreased compared to the representative control (a, d). CSA, cross-sectional area; SPG4, spastic paraplegia type 4; SPG7, spastic paraplegia type 7; $T2_{app}$, apparent T2-relaxation time; T2W, T2 weighted; ρ, proton spin density.

the SPG4 group into SPG4 PNP+ and SPG4 PNP−, differences in tibial nerve CSA were detected at the thigh ($p=0.0129$, $F=4.639$) and the lower leg ($p<0.0001$; $F=13.47$). Post hoc analyses revealed a CSA decrease at the thigh in SPG4 PNP+ versus controls, while differences between SPG4 PNP− and controls as well as between SPG4 PNP+ and SPG4 PNP− did not exist (Table 2 and Figure 5a). At the lower leg, marked reductions in tibial nerve CSA were found in SPG4 PNP+ and in SPG4 PNP− versus controls, but not between SPG4 PNP+ and SPG4 PNP− (Table 2 and Figure 5b). Consistent with the physiologic decrease in nerve caliber from proximal to distal, tibial nerve CSA was markedly higher at the thigh than at the lower leg in all groups ($p<0.0001$, respectively). Side differences in CSA were not observed in SPG4 ($p=0.66$), SPG7 ($p=0.80$), and controls ($p=0.94$).

Tibial nerve CSA at the thigh correlated positively with weight ($r=0.3292$, $p=0.0311$) and BMI ($r=0.3640$, $p=0.0164$) in controls. No further correlations existed.

DISCUSSION

Hereditary spastic paraplegias are a heterogeneous group of rare genetic disorders characterized by length-dependent axonal degeneration mainly of the corticospinal tract leading to progressive weakness and spasticity of the lower limbs [2–4]. However, HSPs are multisystemic diseases that may affect different anatomic regions within the central nervous system (CNS) and peripheral nervous system (PNS) [2–4].

Here, we report on the first comprehensive characterization of lower extremity peripheral nerve involvement in genetically, clinically, and electrophysiologically well-classified HSP SPG4 and SPG7 patients by applying quantitative MRN. Our results show that (i) all four evaluated microstructural and morphometric quantitative MRN parameters are decreased in both HSP groups compared to controls, (ii) peripheral nerve impairment is detectable in SPG4 and SPG7 patients without electrophysiologically manifest PNP, and (iii) ρ is the most sensitive MRN marker allowing the differentiation between subgroups at thigh and lower leg level.

T2-relaxometry has recently gained increasing importance in the development of new imaging biomarkers for diffuse neuropathies and motor neuron diseases [11–13, 17–22]. ρ and $T2_{app}$ are the two quantitative MRN markers generated by T2-relaxometry and provide microstructural information about the integrity, density, and macromolecular composition of central and peripheral nerve tissue in vivo [16, 23, 24]. Recent studies suggest that the direction of change in ρ and $T2_{app}$ is somewhat specific with regard to the underlying disease entity. In detail, distal-symmetric PNPs of different etiologies, such as hereditary or systemic amyloidosis, diabetes, or alcohol dependency, are characterized by an early, often subclinical increase of ρ, followed by an additional $T2_{app}$ increase in symptomatic or more advanced PNP stages [12, 13, 20, 22]. In the demyelinating disease multiple sclerosis (MS), peripheral nerve involvement is characterized by a similar increase in ρ, while $T2_{app}$ is reduced [18, 25]. In the motor neuron disease 5q-linked spinal muscular atrophy (SMA) another unique alteration of MRN markers was observed with a decrease in ρ (and

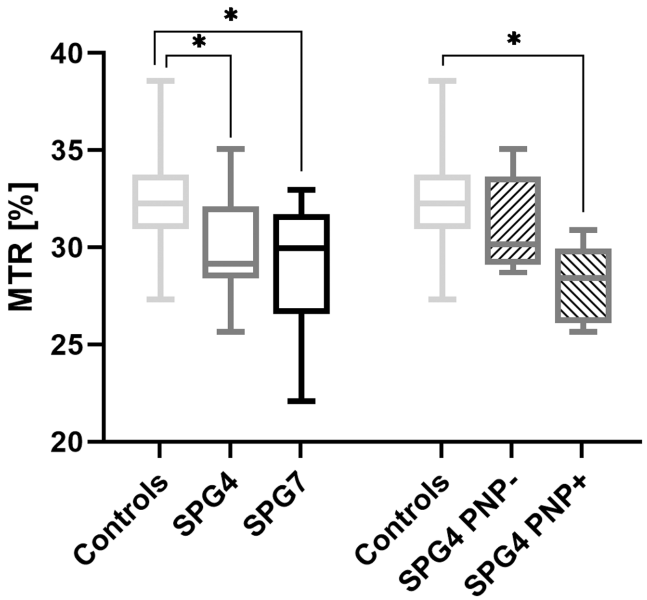

FIGURE 3 Magnetization transfer ratio (MTR). Sciatic nerve MTR mean values at the right mid- to distal thigh were plotted separately for each group in a box and whisker plot. MTR differentiated well between healthy controls and SPG4 as well as between healthy controls and SPG7, while differences between SPG4 and SPG7 were not detected. After subdividing the SPG4 group into patients with and without PNP, MTR separated SPG4 PNP+ patients from controls, while no differences existed between controls and SPG4 PNP− or between SPG4 PNP− and SPG4 PNP+. MTR, magnetization transfer ratio; SPG4 PNP−, spastic paraplegia type 4 patients without polyneuropathy; SPG4 PNP+, spastic paraplegia type 4 patients with polyneuropathy; SPG4 = spastic paraplegia type 4 patients; SPG7, spastic paraplegia type 7 patients. Significant differences are indicated by * = significant ($p \leq 0.05$)).

CSA), likely representing the axonal loss induced by a decay of lower motor neurons, and an increase in $T2_{app}$ potentially caused by reactive nerve edema [11]. Lastly, a recent study in spinocerebellar ataxia type 3 (SCA3), reported a combined decrease in all evaluated quantitative MRN markers, similar to our current findings in HSP [14].

Our results are in line with histopathologic studies that characterize peripheral nerve involvement in HSP as a chronic axonal neuropathy without relevant evidence of regeneration and demyelinisation [26]. This axonal damage is a likely explanation for the observed decrease in ρ, and has been similarly described in other neurodegenerative diseases like SMA or SCA3 [14]. However, contrary to previous observations in SMA, a reactive, potentially edema-induced increase of nerve $T2_{app}$ was absent in SCA3 and HSP. Histopathologic and MRN studies conducted in MS revealed that areas of demyelination in the brain as well as PNS lesions correlate with an increase in ρ [18, 25, 27]. Consequently, the observed decrease in nerve ρ in HSP argues against a relevant demyelination in SPG4 and SPG7, which would rather point towards mimicking immunologic or neurometabolic diseases. In addition, the hypothesis of a chronic degenerative process with predominant axonal loss is supported by the reduced CSA, a sign of nerve atrophy.

Magnetization transfer contrast imaging is another quantitative MRN technique that allows for the visualization of macromolecular bound protons that are not directly measurable by conventional MRI sequences due to their very short T2-relaxation time [28–32]. By using off-resonance pulses to saturate those bound protons, the signal intensity of free protons decreases, enabling the measurement of bound protons by computing the MTR. Only few peripheral neuropathies were previously studied by MTC imaging, but results were promising: In Charcot–Marie–Tooth disease type 1A (CMT1A), nerve MTR was decreased, correlated well with the grade of disability, and provided excellent interscan and interrater reliabilities [33]. Similar results with decreased MTR values were documented in hereditary transthyretin (ATTRv) amyloidosis with PNP, where MTR identified even clinically and electrophysiologically fully asymptomatic carriers of the variant *transthyretin* gene [34]. While it was initially assumed that decreased MTR indicates pure demyelination, it is now accepted that a similar MTR decrease can be observed when axonal density is reduced [28]. This hypothesis is likely the underlying reason for the observed MTR decrease in HSP and is in line with other studies reporting a decreased MTR in SMA or SCA3, both pathomorphologically defined by a predominant axonal loss [14, 35]. In HSP, MTR differentiated well between SPG4 and SPG7 versus controls and between SPG4 PNP+ versus controls, while correlating well with neurophysiologic parameters. One could argue that the observed MTR decrease in several pathophysiologically completely different disease entities indicate low specificity and therewith inferiority of MTR compared to other MRN markers. However, the described positive findings in our cohort underline the high potential of MTR as a sensitive biomarker for the detection of early nerve lesions, potentially allowing the identification of different disease stages. This is particularly interesting since we measured the MTR only at the thigh while group differences in the other MRN markers were even more pronounced when measured at the lower leg.

In our study cohort, seven SPG4 and none of the SPG7 patients fulfilled the electroneurographic criteria for PNP. However, MRN markers, especially ρ, showed a significant decrease in SPG4 with and without PNP as well as in SPG7 compared to controls, indicating that mild or subclinical peripheral nerve involvement is present even when electroneurographic signs of PNP are absent. Furthermore, the observed decrease in ρ, even though not significant between SPG4 PNP− and SPG4 PNP+, appeared to be gradual from controls over SPG4 PNP− to SPG4 PNP+ patients. Additionally, when measuring the morphometric marker CSA at the lower leg, a significant decrease was detected in SPG7 and SPG4 with and without PNP indicating neuronal atrophy, while such a CSA decrease was only detectable for the whole SPG4 group when measured at the thigh. $T2_{app}$ was the weakest parameter and only distinguished controls from SPG7 at the lower leg, while no further group differences were detectable at either anatomic location. Importantly, we found group differences in MRN markers either solely or with higher significance levels at the lower leg, suggesting that peripheral nerve involvement occurs predominantly at the lower leg. This finding in HSP is unique among the

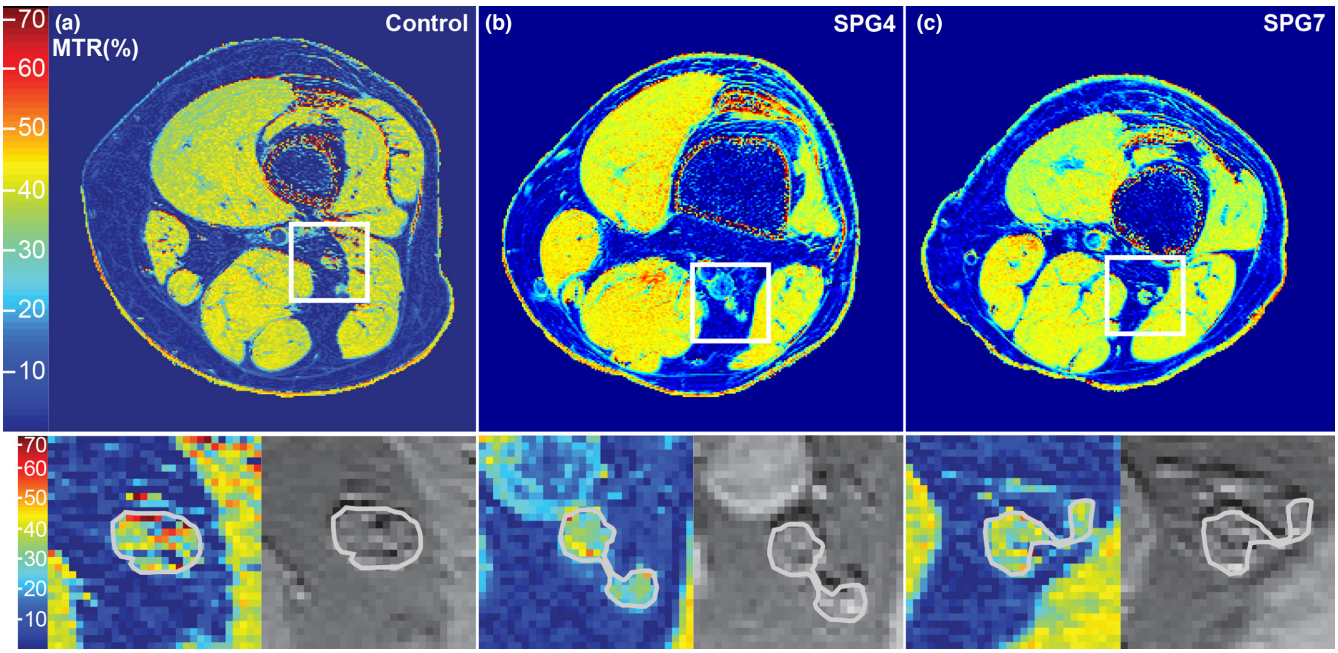

FIGURE 4 Magnetization transfer ratio (MTR) map. Representative MTR pseudo-colorized (%) maps are shown for a healthy control (a), a SPG4 patient (b), and a SPG7 patient (c). The white boxes in a–c are zoomed-in and displayed below to show detailed views of the MTR (%) map (left) and the magnetization transfer contrast (MTC) sequence without the off-resonance pulse (right). The sciatic nerve at the right mid-thigh is encircled in white. Note the marked decrease of sciatic nerve MTR (%) in SPG4 (b) and SPG7 (c; loss of red and yellow signals) compared to the healthy control (a). SPG4, spastic paraplegia type 4; SPG7, spastic paraplegia type 7.

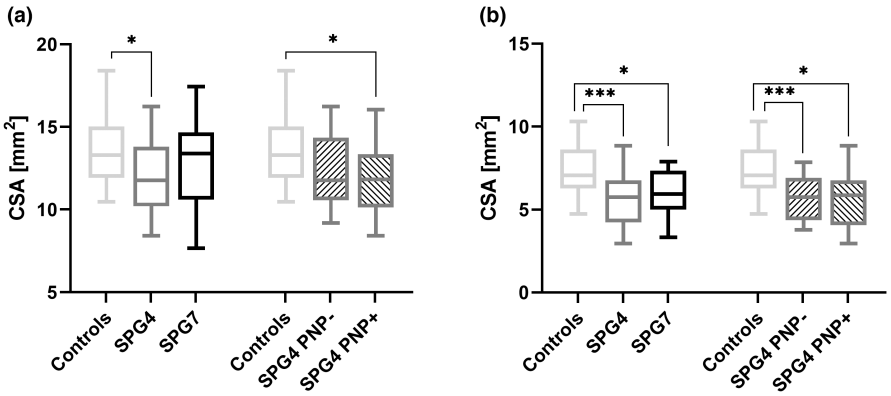

FIGURE 5 Cross-sectional area (CSA). Tibial nerve CSA mean values at thigh level (a) and at the lower leg (b) were plotted separately for each group in a box and whisker plot. At the thigh, tibial nerve CSA differentiated only between healthy controls and SPG4 patients, but not between controls and SPG7 or between SPG4 and SPG7. At the lower leg, CSA differentiated SPG4 and SPG7 patients from healthy controls. In addition, tibial nerve CSA separated SPG4 PNP+ patients from healthy controls at both the thigh and the lower leg. At the lower leg, CSA differentiated also between SPG4 PNP− and controls. CSA, cross-sectional area; SPG4 PNP−, spastic paraplegia type 4 patients without polyneuropathy; SPG4 PNP+, spastic paraplegia type 4 patients with polyneuropathy; SPG4, spastic paraplegia type 4 patients; SPG7, spastic paraplegia type 7 patients. Significant differences are indicated by either * = significant ($p \leq 0.05$) or *** = highly significant ($p \leq 0.001$).

diffuse neuropathies characterized by MRN to date, as a proximal rather than a distal dominant MRN marker change was described in other entities [12–14, 20–22, 25]. Furthermore, the presumably distal predominance of microstructural changes in the extracellular nerve matrix might explain our finding that MTR (measured only at the thigh) failed to detect nerve involvement in SPG4 PNP−, even though it previously showed superiority in identifying subclinical nerve damage in other neuropathies.

Quantitative MRN markers correlated well with clinical markers, not only with regard to clinical signs reflecting PNP-like pallhypesthesia ($T2_{app}$), but also with regard to disease duration and the SPRS score (ρ and $T2_{app}$) [15]. The described correlations are particularly relevant as MRN parameters are objective, quantifiable, and analyzable by an observer blinded to clinical data. In contrast, clinical rating scales can be influenced by day shape-dependent fluctuations in clinical symptoms or by the observers´ overall clinical impression of

a patient. Additionally, correlation of $T2_{app}$ and MTR with electroneurographic results in SPG7 and SPG4, even without electroneurographic signs of PNP, indicate subclinical changes not only in nerve microstructure but also in electric conductivity. Therewith, the objectivity of quantitative MRN is an important advantage and makes respective MRN markers promising outcome parameters even in early disease stages.

An important limitation of our study is its cross-sectional design, not allowing conclusions about the temporal development of structural nerve damage. Future longitudinal studies are needed to clarify whether quantitative MRN parameters can be reliable imaging biomarkers of disease progression. Furthermore, sex is a potential confounder of nerve CSA, while no influence exists on ρ, $T2_{app}$, and MTR [31, 36]. Even though our study results point against it, the unequal sex distribution in most of our subgroups could have potentially influenced our CSA results. Another limitation is the restriction to just two representative genotypes. However, given the extreme heterogeneity of HSPs with >100 genetically defined subtypes affecting children and adults, we decided to focus only on adult patients with SPG4 and SPG7 as two common subtypes of HSP. Therefore, it is impossible to draw conclusions about other subtypes or age groups. Furthermore, typical challenges of pediatric imaging such as patient motion and lack of cooperation, especially when long examination times are needed, may limit the application of MRN in children.

Our study results provide an important characterization of peripheral nerve involvement in SPG4 and SPG7 that might help to understand the mechanisms involved in the multisystemic disease evolution in HSP. The combined decrease in all evaluated quantitative MRN markers strengthens the hypothesis of an axonal loss as the main pathomorphologic change in HSP, while the noticeable involvement of lower leg nerves supports the hypothesis of a length-dependent neurodegeneration leading to axonal damage. While group differences between SPG4 and SPG7 versus controls were detectable with most quantitative MRN markers, ρ was most suitable to identify mild structural nerve changes in SPG4 and SPG7 patients without electrophysiologically manifest PNP. The detection of a peripheral nerve involvement in all subgroups challenges the current view that pure HSPs with isolated pyramidal signs exist. Correlation of MRN markers with clinical measures of disease severity further support their potential as progression biomarkers in HSP.

AUTHOR CONTRIBUTIONS

Heike Jacobi: Conceptualization; investigation; writing – original draft; methodology; validation; formal analysis; project administration; data curation; supervision; funding acquisition. **Markus Weiler:** Investigation; methodology; validation; formal analysis; data curation. **Georges Sam:** Investigation; validation; formal analysis; data curation. **Sabine Heiland:** Investigation; methodology; validation; software; formal analysis; data curation; supervision; funding acquisition; resources. **John Hayes:** Methodology; validation; visualization; software; formal analysis; data curation. **Martin Bendszus:** Methodology; validation; software; formal analysis; resources; data curation; supervision; funding acquisition. **Rebecca Schüle:** Conceptualization; methodology; validation; data curation. **Jennifer C. Hayes:** Conceptualization; investigation; methodology; visualization; validation; writing – original draft; software; formal analysis; project administration; data curation; supervision; funding acquisition; resources. Statistical analyses conducted by Jennifer C. Hayes, MD.

ACKNOWLEDGEMENTS

Open Access funding enabled and organized by Projekt DEAL.

FUNDING INFORMATION

The study was supported in part by the Medical Faculty of the University of Heidelberg (Olympia Morata stipend grant to H.J.), the German Research Foundation (SFB 1118 to S.H., SFB 1158 to M.B.), and Alnylam Pharmaceuticals (grant to J.C.H.) and the Bundesministerium für Forschung und Bildung (BMBF) through funding for the TreatHSP network (grant 01GM1905) (to R.S.).

CONFLICT OF INTEREST STATEMENT

H.J. received the Olympia Morata stipend grant from the Medical Faculty of the University of Heidelberg. M.W. reports no disclosures relevant to this work. G.S. reports no disclosures relevant to this work. S.H. received research grants from the German Research Foundation (SFB 1118). J.M.H. reports no disclosures relevant to this work. M.B. reports personal fees from Boehringer Ingelheim; grants and personal fees from Novartis and Guerbet; grants from Siemens, the Hopp Foundation, the German Research Foundation (SFB 1158), the European Union, and Stryker; personal fees from Merck, Bayer, Teva, BBraun, Vascular Dynamics, Grifols, and Neuroscios. R.S. reports grants from the Bundesministerium für Forschung und Bildung (BMBF) through funding for the TreatHSP network (grant 01GM1905), the German Center for Neurodegenerative Diseases (DZNE), and is a member of the European Reference Network for Rare Neurological Diseases (Project ID 739510). J.C.H. reports no disclosures relevant to this work.

DATA AVAILABILITY STATEMENT

The data that support the findings of this study are available from the corresponding author upon reasonable request.

ORCID

Heike Jacobi https://orcid.org/0000-0002-6986-3969

REFERENCES

1. Erfanian Omidvar M, Torkamandi S, Rezaei S, et al. Genotype-phenotype associations in hereditary spastic paraplegia: a systematic review and meta-analysis on 13,570 patients. *J Neurol*. 2021;268:2065-2082.
2. Harding AE. Hereditary "pure" spastic paraplegia: a clinical and genetic study of 22 families. *J Neurol Neurosurg Psychiatry*. 1981;44:871-883.

3. Harding AE. Classification of the hereditary ataxias and paraplegias. *Lancet*. 1983;1:1151-1155.
4. Harding AE. Hereditary spastic paraplegias. *Semin Neurol*. 1993;13:333-336.
5. Salinas S, Proukakis C, Crosby A, Warner TT. Hereditary spastic paraplegia: clinical features and pathogenetic mechanisms. *Lancet Neurol*. 2008;7:1127-1138.
6. de Souza PVS, de Rezende Pinto WBV, de Rezende Batistella GN, Bortholin T, Oliveira ASB. Hereditary spastic paraplegia: clinical and genetic hallmarks. *Cerebellum*. 2017;16:525-551.
7. Kumar KR, Sue CM, Burke D, Ng K. Peripheral neuropathy in hereditary spastic paraplegia due to spastin (SPG4) mutation – a neurophysiological study using excitability techniques. *Clin Neurophysiol*. 2012;123:1454-1459.
8. Orlacchio A, Kawarai T, Gaudiello F, et al. Clinical and genetic study of a large SPG4 Italian family. *Mov Disord*. 2005;20:1055-1059.
9. Schulte T, Miterski B, Bornke C, Przuntek H, Epplen JT, Schols L. Neurophysiological findings in SPG4 patients differ from other types of spastic paraplegia. *Neurology*. 2003;60:1529-1532.
10. Jende JME, Groener JB, Oikonomou D, et al. Diabetic neuropathy differs between type 1 and type 2 diabetes: insights from magnetic resonance neurography. *Ann Neurol*. 2018;83:588-598.
11. Kollmer J, Hilgenfeld T, Ziegler A, et al. Quantitative MR neurography biomarkers in 5q-linked spinal muscular atrophy. *Neurology*. 2019;93:e653-e664.
12. Kollmer J, Hund E, Hornung B, et al. In vivo detection of nerve injury in familial amyloid polyneuropathy by magnetic resonance neurography. *Brain*. 2015;138:549-562.
13. Pham M, Oikonomou D, Hornung B, et al. Magnetic resonance neurography detects diabetic neuropathy early and with proximal predominance. *Ann Neurol*. 2015;78:939-948.
14. Kollmer J, Weiler M, Sam G, et al. Quantitative magnetic resonance neurographic characterization of peripheral nerve involvement in manifest and pre-ataxic spinocerebellar ataxia type 3. *Eur J Neurol*. 2022;29:1782-1790.
15. Schule R, Holland-Letz T, Klimpe S, et al. The spastic paraplegia rating scale (SPRS): a reliable and valid measure of disease severity. *Neurology*. 2006;67:430-434.
16. Heiland S, Sartor K, Martin E, Bardenheuer HJ, Plaschke K. In vivo monitoring of age-related changes in rat brain using quantitative diffusion magnetic resonance imaging and magnetic resonance relaxometry. *Neurosci Lett*. 2002;334:157-160.
17. Poncelet A, Weiler M, Hegenbart U, et al. Dual-echo turbo spin echo and 12-echo multi spin echo sequences as equivalent techniques for obtaining T2-relaxometry data: application in symptomatic and asymptomatic hereditary transthyretin amyloidosis as a surrogate disease. *Invest Radiol*. 2022;57:301-307.
18. Jende JME, Hauck GH, Diem R, et al. Peripheral nerve involvement in multiple sclerosis: demonstration by magnetic resonance neurography. *Ann Neurol*. 2017;82:676-685.
19. Kollmer J, Sahm F, Hegenbart U, et al. Sural nerve injury in familial amyloid polyneuropathy: MR neurography vs clinicopathologic tools. *Neurology*. 2017;89:475-484.
20. Kollmer J, Weiler M, Purrucker J, et al. MR neurography biomarkers to characterize peripheral neuropathy in AL amyloidosis. *Neurology*. 2018;91:e625-e634.
21. Kollmer J, Bendszus M. Magnetic resonance neurography: improved diagnosis of peripheral neuropathies. *Neurotherapeutics*. 2021;18:2368-2383.
22. Rother C, Bumb JM, Weiler M, et al. Characterization and quantification of alcohol-related polyneuropathy by magnetic resonance neurography. *Eur J Neurol*. 2022;29:573-582.
23. Miot E, Hoffschir D, Alapetite C, et al. Experimental MR study of cerebral radiation injury: quantitative T2 changes over time and histopathologic correlation. *AJNR Am J Neuroradiol*. 1995;16:79-85.
24. Walimuni IS, Hasan KM. Atlas-based investigation of human brain tissue microstructural spatial heterogeneity and interplay between transverse relaxation time and radial diffusivity. *Neuroimage*. 2011;57:1402-1410.
25. Pietsch AM, Viehover A, Diem R, et al. Quantification and proximal-to-distal distribution pattern of tibial nerve lesions in relapsing-remitting multiple sclerosis: assessment by MR neurography. *Clin Neuroradiol* 2022. doi: 10.1007/s00062-022-01219-1.
26. Kara E, Tucci A, Manzoni C, et al. Genetic and phenotypic characterization of complex hereditary spastic paraplegia. *Brain*. 2016;139:1904-1918.
27. Nijeholt GJ, Bergers E, Kamphorst W, et al. Post-mortem high-resolution MRI of the spinal cord in multiple sclerosis: a correlative study with conventional MRI, histopathology and clinical phenotype. *Brain*. 2001;124:154-166.
28. Does MD, Beaulieu C, Allen PS, Snyder RE. Multi-component T1 relaxation and magnetisation transfer in peripheral nerve. *Magn Reson Imaging*. 1998;16:1033-1041.
29. Kollmer J, Kastel T, Jende JME, Bendszus M, Heiland S. Magnetization transfer ratio in peripheral nerve tissue: does it depend on age or location? *Invest Radiol*. 2018;53:397-402.
30. Wolff SD, Balaban RS. Magnetization transfer contrast (MTC) and tissue water proton relaxation in vivo. *Magn Reson Med*. 1989;10:135-144.
31. Fosleitner O, Schwehr V, Godel T, et al. Magnetization transfer ratio of peripheral nerve and skeletal muscle: correlation with demographic variables in healthy volunteers. *Clin Neuroradiol*. 2022;32:557-564.
32. McGowan JC. The physical basis of magnetization transfer imaging. *Neurology*. 1999;53:S3-S7.
33. Dortch RD, Dethrage LM, Gore JC, Smith SA, Li J. Proximal nerve magnetization transfer MRI relates to disability in Charcot-Marie-tooth diseases. *Neurology*. 2014;83:1545-1553.
34. Kollmer J, Hegenbart U, Kimmich C, et al. Magnetization transfer ratio quantifies polyneuropathy in hereditary transthyretin amyloidosis. *Ann Clin Transl Neurol*. 2020;7:799-807.
35. Kollmer J, Kessler T, Sam G, et al. Magnetization transfer ratio: a quantitative imaging biomarker for 5q spinal muscular atrophy. *Eur J Neurol*. 2021;28:331-340.
36. Kronlage M, Schwehr V, Schwarz D, et al. Magnetic resonance neurography: normal values and demographic determinants of nerve caliber and T2 relaxometry in 60 healthy individuals. *Clin Neuroradiol*. 2019;29:19-26.

SUPPORTING INFORMATION

Additional supporting information can be found online in the Supporting Information section at the end of this article.

How to cite this article: Jacobi H, Weiler M, Sam G, et al. Peripheral nerve involvement in hereditary spastic paraplegia characterized by quantitative magnetic resonance neurography. *Eur J Neurol*. 2023;30:2442-2452. doi:10.1111/ene.15841